

Dissipative structures in optomechanical cavities

Joaquín Ruiz-Rivas,¹ Carlos Navarrete-Benlloch,² Giuseppe Patera,³ Eugenio Roldán,¹ and Germán J. de Valcárcel¹

¹*Departament d'Òptica, Universitat de València, Dr. Moliner 50, 46100 Burjassot, Spain*

²*Max-Planck Institut für Quantenoptik, Hans-Kopfermann-Str. 1, D-85748 Garching, Germany*

³*Laboratoire de Physique des Lasers, Atomes et Molécules,
Université Lille 1, 59655 Villeneuve d'Ascq Cedex, France*

We analyze the possibility of pattern formation in an optical cavity in which one of its mirrors can be deformed by radiation pressure. Our model treats the deformable mirror as tense membrane that can oscillate, not only back and forth around its axial equilibrium position (center of mass motion), but also in its transverse degrees of freedom, vibrating like a drum in combinations of modes. We demonstrate the existence of periodic patterns and localized structures (cavity solitons) in this model, which should be realizable with current technology.

PACS numbers: 42.65.Sf, 42.50.Wk, 07.10.Cm

Introduction. Since the eighties of the past century, the advent and rapid growing of the field of quantum information have boosted the research on quantum technologies that try to develop nano and microdevices allowing for robust implementations of controllable quantum interactions, together with long coherence times. By today the state of the art permits the fabrication of devices functioning in such strong coupling regime with unprecedented control and accuracy. These new quantum devices are very diverse including cavity-QED [1], optical lattices [2], trapped ions [3], superconducting circuits [4], quantum dots [5], atomic ensembles [6], optomechanical devices [7], etc.

In optomechanical systems [7] the interaction occurs between a light field and a mechanical oscillator via radiation pressure. These type of systems have been known for a long time in, say, macroscopic optics [8], and to some extent resemble a nonlinear Kerr cavity [9] as the cavity length (and consequently the cavity resonance) depends on the intracavity field intensity. At present, the stress is made on their capability to show quantum coherent phenomena such as cooling and amplification [10], or strong (linear) coupling effects like optomechanically induced transparency [11]. Attention has also been recently paid to the nonlinear dynamics of optomechanical arrays [12], cavities in which radiation pressure competes with the photothermal effect [13], planar dual-nanoweb waveguides subject to radiation pressure [14], and optomechanical cavities containing atomic ensembles [15].

Except for some of these recent works, up to now most of the studies have considered a small number of modes either in the radiation or the mechanical fields. However multimode configurations can provide optomechanical systems with new capabilities, as the nonlinear interplay between many optical and mechanical modes entails the existence of correlations between them. At the quantum level, these correlations may lead to multipartite entanglement [16–18]. At the classical level, they help for the spontaneous appearance of dissipative structures that are long range ordered field configurations, including

periodic and quasiperiodic patterns as well as localized structures [19], which may even exhibit nontrivial temporal behavior.

The interplay between the quantum and classical perspectives in multimode systems has received theoretical attention in the past mainly in the context of optical parametric oscillators, and some exciting phenomena have been predicted [20]. However no such studies exist concerning optomechanical systems.

Here we address the modeling of pattern formation in an optomechanical oscillator. We will keep our study at the classical level by concentrating on the analysis of the general conditions under which nonlinear patterns can appear and how these patterns are, and leave the study of their quantum properties for a future publication. As we show below, periodic patterns and localized structures (cavity solitons) are predicted in both 1 and 2 transverse dimensions in a wide region of the parameter space.

The model. Consider an optical cavity with large-area mirrors one of which is plane, partially transmitting, and immune to radiation pressure because of its stiffness and mass, while the other is a perfectly reflecting deformable mirror. The latter can be thought of as a tense membrane that can oscillate, forced by the intracavity radiation pressure, not only back and forth around its axial equilibrium position (center of mass motion) but also in its transverse degrees of freedom, vibrating like a drum in combinations of modes. The movement of the center of mass will be modeled as a homogeneous mode (independent of the transverse coordinates) while the modes deforming the flatness of the mirror will be modeled as the nondispersive surface waves occurring in a tense membrane. Energy is fed in the cavity from the outside by injecting a coherent laser beam through the partially transmitting mirror. We denote by $z = 0, L$ the planes containing the coupling mirror and the surface of the deformable mirror at rest (i.e., in the absence of illumination), respectively. Find a sketch of the system in Fig. 1.

The field injected in the cavity through the coupling

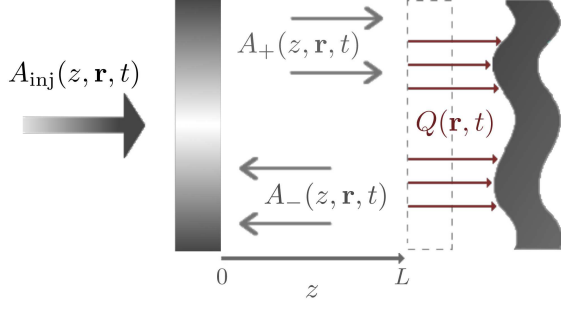


FIG. 1: Cartoon of the optomechanical system studied in this Letter.

mirror will be considered to be a paraxial, coherent beam of the form

$$E_{\text{inj}}(z, \mathbf{r}, t) = i\mathcal{V}A_{\text{inj}}(z, \mathbf{r}, t)e^{i(k_L z - \omega_L t)} + \text{c.c.}, \quad (1)$$

where $\mathbf{r} = (x, y)$ denotes the position in the plane transverse to the cavity axis (z -axis), and \mathcal{V} is a constant having the dimensions of voltage. The intracavity field $E(z, \mathbf{r}, t)$ can be written generically as

$$E(z, \mathbf{r}, t) = i\mathcal{V}(A_+e^{ik_L z} + A_-e^{-ik_L z})e^{-i\omega_L t} + \text{c.c.}, \quad (2)$$

which is the superposition of two waves of complex amplitudes $A_{\pm}(z, \mathbf{r}, t)$, propagating along the positive (A_+) and negative (A_-) z direction. Our first goal is to derive an evolution equation for the amplitude $A_+(z=L, \mathbf{r}, t)$ at the deformable mirror surface, which we will denote by $A(\mathbf{r}, t)$ [21]. The procedure follows the lines of [22] and consists in propagating the complex amplitude along a full cavity roundtrip, which, under reasonable assumptions (see the supplemental material for details) leads to

$$\partial_t A = \gamma_c \left(-1 + i\Delta + il_c^2 \nabla_{\perp}^2 + i\frac{4k_L}{T}Q \right) A + \gamma_c \mathcal{E}, \quad (3)$$

where γ_c is the cavity damping rate, $\Delta = (\omega_L - \omega_c)/\gamma_c$ is the dimensionless detuning parameter (ω_c is the frequency of the longitudinal cavity mode closest to ω_L), l_c is the diffraction length, $\nabla_{\perp}^2 = \partial_x^2 + \partial_y^2$ is the transverse Laplacian, $Q(\mathbf{r}, t)$ is the displacement of the mirror perpendicular to its flat state ($Q=0$ at rest), T is the transmissivity of the fixed mirror, and $\mathcal{E}(\mathbf{r}, t)$ is a scaled version of the injection field amplitude.

The equation for the light field must be complemented with an equation for the displacement field $Q(\mathbf{r}, t)$. In the absence of forcing and dissipation Q obeys a wave equation $\partial_t^2 Q + \mathbb{L}Q = 0$, where \mathbb{L} is a suitable differential operator. It is useful to diagonalize the problem by introducing a set of normal modes $\{u_j(\mathbf{r})\}_{j=0}^{\infty}$, which are the solutions to the linear problem $\mathbb{L}u_j(\mathbf{r}) = \tilde{\Omega}_j^2 u_j(\mathbf{r})$ subject to appropriate boundary conditions; here $\tilde{\Omega}_j$ is the mode j frequency. Without loss of generality we take the normal modes as dimensionless functions of \mathbf{r} , which

we choose to be normalized as

$$\int_S d^2\mathbf{r} u_j(\mathbf{r}) u_l^*(\mathbf{r}) = \delta_{jl} m_j / \sigma, \quad (4)$$

where S is the mirror surface, σ is its surface mass density, and m_j is the so-called effective mass [23] which won't play any relevant role in our case. As usual [23], the displacement field is expanded onto the normal mode basis as

$$Q(\mathbf{r}, t) = \sum_j q_j(t) u_j(\mathbf{r}), \quad (5)$$

and then the generalized coordinates q_j are modeled as damped harmonic oscillators forced by radiation pressure:

$$\ddot{q}_j + \gamma_j \dot{q}_j + \tilde{\Omega}_j^2 q_j = F_j / m_j. \quad (6)$$

In this equation γ_j is a damping rate and the radiation pressure force can be written as

$$F_j(t) = \frac{2\hbar k_c}{t_c} \int_S d^2\mathbf{r} |A(\mathbf{r}, t)|^2 u_j^*(\mathbf{r}), \quad (7)$$

with $t_c = 2L/c$ the cavity roundtrip time. In writing F_j we used the expression for the radiation pressure on the movable mirror $P_{\text{rad}}(\mathbf{r}, t) = \langle S_+(\mathbf{r}, t) \rangle / c$ in terms of the time averaged modulus of the Poynting vector associated to the wave impinging the deformable mirror, which in our notation reads $\langle S_+ \rangle = 2\varepsilon_0 c \mathcal{V}^2 |A|^2$ [24].

Up to here the treatment is general. In order to obtain an evolution equation for $Q(\mathbf{r}, t)$ a specific model for the mirror dynamics must be chosen, both for its Hamiltonian part, governed by the differential operator \mathbb{L} , and for its dissipative part. Here we choose the simplest $\mathbb{L} = \tilde{\Omega}_0^2 - v^2 \nabla_{\perp}^2$, which models a membrane (characterized by its sound velocity v) that can oscillate as a whole (the homogeneous mode) at a frequency $\tilde{\Omega}_0$. This situation could be implemented experimentally by attaching the membrane to a compressible substrate. Certainly, if the mirror is mounted on a fixed frame the displacement field $Q(\mathbf{r}, t)$ cannot possess a homogeneous mode, but our choice would still be a reasonable approximation valid for large mirrors as compared to the transverse size of the optical beam, and low light intensities (which induce small deformations in the mirror), similarly to what happens in cavities with nonlinear elements [25]. With this choice the normal modes are 2D plane waves $\exp(i\boldsymbol{\kappa} \cdot \mathbf{r})$, specified by a (transverse) wave vector $\boldsymbol{\kappa}$, with associated frequencies $\tilde{\Omega}_{\boldsymbol{\kappa}}^2 = \tilde{\Omega}_0^2 + v^2 \kappa^2$, being $\kappa = |\boldsymbol{\kappa}|$. As for the dissipative dynamics we assume the simplest case of equal losses $\gamma_{\boldsymbol{\kappa}} = \gamma_m$ for all modes, so that using Eqs. (4)-(7) one readily obtains

$$\partial_t^2 Q + \gamma_m \partial_t Q + \left(\tilde{\Omega}_0^2 - v^2 \nabla_{\perp}^2 \right) Q = \frac{2\hbar k_c}{\sigma t_c} |A|^2. \quad (8)$$

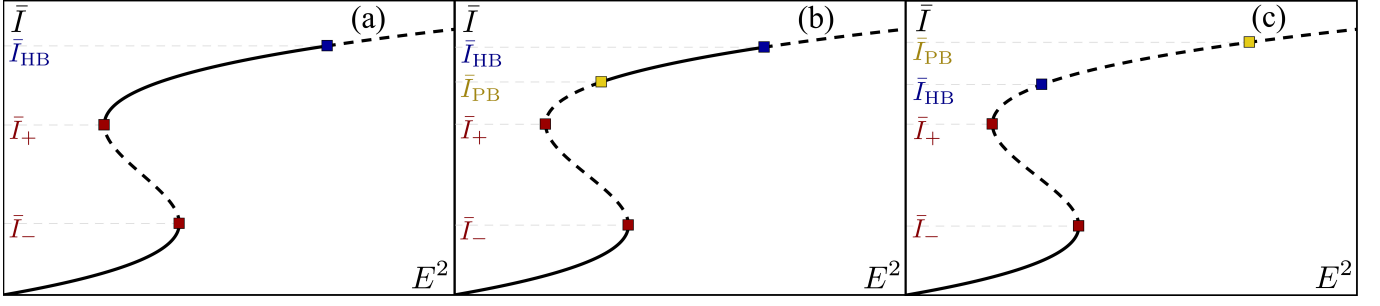


FIG. 2: Illustration of the system's instabilities. We plot the intensity \bar{I} of the homogeneous steady-state solution as a function of the injection E^2 (both quantities are in arbitrary units), with the stable (unstable) regions denoted by solid (dashed) lines. We mark with squares both turning points, as well as the Hopf instability leading to oscillatory solutions and the Pitchfork instability leading to pattern formation. As explained in the text, three relevant scenarios can be found as the detuning is decreased from $\Delta = -2$ (assuming $\rho > 1$ and small mechanical losses): absence of the Pitchfork bifurcation for Δ above some threshold Δ_0 (a), and presence of the Pitchfork bifurcation before (b) or after (c) the Hopf instability. For small rigidities ($\rho \leq 1$), the scenario is like (c), but with the Pitchfork bifurcation going to infinity, irrespective of the value of the detuning.

Equations (3) and (8) constitute our optomechanical cavity model. Before continuing however, and in order to give a cleaner presentation, we introduce normalized and dimensionless time $\tau = \gamma_c t$ and spatial coordinates $\mathbf{r}' = \mathbf{r}/l_c$, together with the variables and parameters

$$Z = \frac{4k_L}{T}Q, \quad F = \frac{2}{\tilde{\Omega}_0} \sqrt{\frac{2\hbar k_c k_L}{t_c \sigma T}} A, \quad \mathbf{k} = l_c \boldsymbol{\kappa}, \quad (9)$$

$$E = \frac{2}{\tilde{\Omega}_0} \sqrt{\frac{2\hbar k_c k_L}{t_c \sigma T}} \mathcal{E}, \quad \Omega_0 = \frac{\tilde{\Omega}_0}{\gamma_c}, \quad \gamma = \frac{\gamma_m}{\gamma_c}.$$

Using Eqs. (3) and (8) we get

$$\partial_\tau F = (-1 + i\Delta + i\nabla^2 + iZ) F + E, \quad (10a)$$

$$\partial_\tau^2 Z + \gamma \partial_\tau Z + \Omega_0^2 (1 - \rho^2 \nabla^2) Z = \Omega_0^2 |F|^2, \quad (10b)$$

where $\nabla^2 = l_c^2 (\partial_x^2 + \partial_y^2) = (\partial_{x'}^2 + \partial_{y'}^2)$, and we defined the 'effective rigidity parameter'

$$\rho = v/\tilde{\Omega}_0 l_c, \quad (11)$$

so that the larger ρ the more rigid the mirror behaves. Alternatively ρ is a measure of how local the response of the vibrating membrane is to a stress: when $\rho \rightarrow 0$ the response is local while for $\rho \rightarrow \infty$ it is completely integrated, that is, only the homogeneous mode is excited. Note finally that in the (just mathematical) limit $\gamma \rightarrow \infty$ and $\rho \rightarrow 0$, the mirror field can be adiabatically eliminated as $Z = |F|^2$ and our model reduces to that of the self-focusing Kerr cavity [9].

Homogeneous solutions and their stability.

When the injected field is a monochromatic plane wave propagating along the cavity axis, the amplitude E is a constant, which we take as real and positive without loss of generality (this just sets the reference phase). In such a case (10) admits spatially homogeneous, steady solutions, which verify $\bar{Z} = |\bar{F}|^2 \doteq \bar{I}$ (in the following an

overbar denotes the homogeneous steady state), with

$$E^2 = \left[1 + (\Delta + \bar{I})^2\right] \bar{I}. \quad (12)$$

The above is the usual state equation of the single-mode pendular cavity (or of a Kerr cavity), which predicts single-valued (three-valued) response for $\Delta > -\sqrt{3}$ ($\Delta < -\sqrt{3}$). In the latter case the characteristic $\bar{I} - E^2$ curve exhibits the well known S-shape (Fig. 2), with the turning points located at $\bar{I}_\pm = (-2\Delta \pm \sqrt{\Delta^2 - 3})/3$. In the following we will use \bar{I} instead of E as a control parameter because \bar{I} fixes the steady state and determines univocally the value of E through (12), not the other way around.

This spatially homogeneous steady state can suffer different instabilities, or bifurcations, leading to the appearance of new type of solutions, such as time-periodic solutions or spatial patterns. In the supplemental material we explain how to find these instabilities through a standard linear stability analysis in which one studies the evolution of small perturbations around the steady solution. Indeed, we have classified all the possible instabilities by using the Routh-Hurwitz criterion [26] and have found that spatial patterns and optomechanical cavity solitons can appear under a large variety of situations. However, since our goal in this Letter is showing that pattern formation is possible by means of optomechanical coupling, we focus on a region of the parameter space where the instabilities can be summarized in a simple fashion, leaving the exhaustive analysis for a future publication. Hence we concentrate in the following on the experimentally relevant limit $\gamma \ll \Omega_0$ (the mechanical oscillations are of high- Q) and $\gamma \ll 1$ (the damping rate of the mirror oscillations is much smaller than the cavity damping rate). As well we restrict our presentation to negative values of Δ (red detuned injection), in particular to $\Delta < -2$, as this is the detuning domain where the analysis is more transparent.

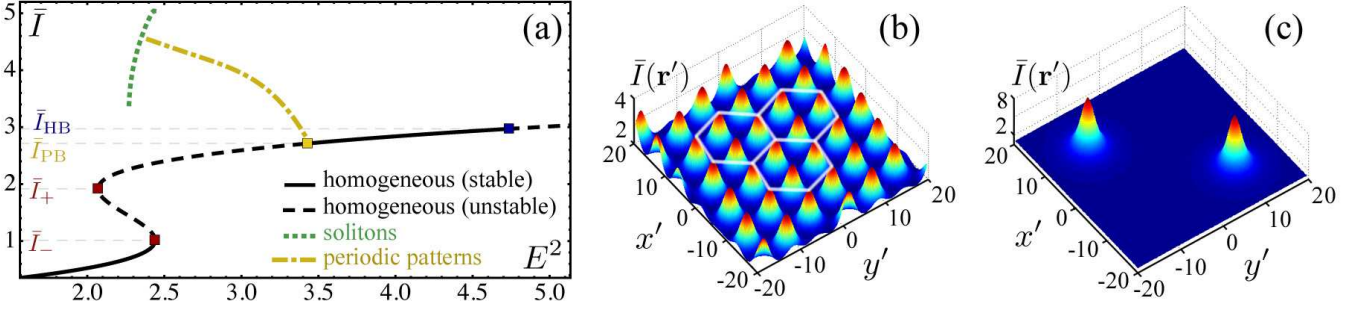


FIG. 3: (a) Same as Fig. 2 for the parameters of the numerical simulation $\Delta = -2.2$, $\gamma = 0.1$, $\Omega_0 = 10$, and $\rho = 1.13$. We have found two types of patterns: periodic (hexagonal in 2D) patterns (b), whose average intensity (half the sum of their maximum and minimum) is represented as a yellow, dashed-dotted line in their domain of existence; and solitons (c), represented as a green, dotted line. Above the Hopf instability we find homogeneous, time-periodic solutions (not represented in the figure).

In the considered detuning domain $\Delta < -2$ the S-shaped response is present. We find that the lower branch of the characteristic $\bar{I} - E^2$ curve is stable in all cases, while the middle branch is intrinsically unstable, as usual. As for the upper branch, it is always affected by a homogeneous Hopf bifurcation, which occurs at an intracavity intensity \bar{I}_{HB} , the steady state being unstable for $\bar{I} > \bar{I}_{\text{HB}}$, see Fig. 2. The expression for \bar{I}_{HB} is lengthy, but in the considered limit $\gamma \ll 1$ we find

$$2\bar{I}_{\text{HB}} = \sqrt{\Delta^2 + \gamma(1 + \Omega_0)^2 / \Omega_0^2} - \Delta. \quad (13)$$

On the other hand, and this is the interesting point, a static, pattern forming instability exists that affects the upper branch. It occurs at an intracavity intensity \bar{I}_{PB} (whose analytic expression is too lengthy to be given here) and the steady state is unstable for $\bar{I}_+ < \bar{I} < \bar{I}_{\text{PB}}$; hence this instability acts oppositely to the Hopf, see Fig. 2(b). For $\rho > 1$ the instability exists for $-\infty < \Delta < \Delta_0$, where Δ_0 is the only real (and negative) solution to

$$\rho^2 = 3 \frac{2\sqrt{\Delta_0^2 - 3} - \Delta_0}{3 + \Delta_0 (\Delta_0 + \sqrt{\Delta_0^2 - 3})}. \quad (14)$$

Just at $\Delta = \Delta_0$ the bifurcation is located at the upper turning point ($\bar{I}_{\text{PB}} = \bar{I}_+$) and as we depart more from resonance (i.e. by making Δ more negative) it climbs through the upper branch, eventually entering the region which is already Hopf unstable ($\bar{I}_{\text{PB}} > \bar{I}_{\text{HB}}$), see Fig. 2(c). As the rigidity ρ is decreased ($\rho \rightarrow 1^+$), $\bar{I}_{\text{PB}} \rightarrow \infty$ and for $\rho < 1$ the whole upper branch is unstable against spatial perturbations irrespective of Δ . Hence three basic scenarios exist in the considered limit ($\gamma \ll \Omega_0, 1$; $\Delta < -2$), depending on the relative position of the two bifurcations, as depicted in Fig. 2.

We conclude that pattern formation is favored by small rigidities, as expected, or by large (negative) detunings.

Numerical integration of the model equations. The linear stability analysis so far presented cannot inform us about the type of patterns appearing once the

bifurcation is crossed, hence a numerical analysis is necessary. We shall concentrate on the static patterns appearing at low intensities (below the Hopf bifurcation), under the conditions specified above, leaving the analysis of the dynamic patterns for future work. We have numerically integrated the model Eqs. (10) in 1D and 2D by using the split-step method for the special parameter choice $\gamma = 0.1$, $\Omega_0 = 10$, $\Delta = -2.2$, and $\rho = 1.13$. In this case $\Delta < \Delta_0 = -1.75847$, and then the upper branch of the steady homogeneous solution has a finite domain of stability for $\bar{I} \in [\bar{I}_{\text{PB}}, \bar{I}_{\text{HB}}]$, as in Fig. 2(b). In Fig. 3(a) we represent the characteristic curve $\bar{I} - E^2$, together with the average intensity corresponding to the different patterned solutions we have found. The patterns are of two types: periodic patterns, which are hexagons in the 2D case, see Fig. 3(b), and localized structures, see Fig. 3(c). We have checked that these localized structures are actual cavity solitons (CS): (i) they can be written and erased (by using appropriate injected pulses) at any point, (ii) when several solitons are present, the deletion of one does not affect the rest, and (iii) they can be moved across the transverse plane by using, e.g. phase gradients of the injected field.

We would like to remark that in the $\bar{I}_{\text{PB}} > \bar{I}_{\text{HB}}$ case corresponding to Fig. 2(c), the pattern formation scenario is similar, except for the fact that the patterns may start pulsing in vicinity of the Hopf bifurcation.

Conclusions. We have proposed a model for pattern formation in an optomechanical system. Our model considers a cavity formed by a fixed rigid mirror and an oscillating deformable mirror. We have simplified the description of the latter by assuming the existence of a homogeneous oscillating mode together with mechanical waves (modeled as those of a vibrating membrane), proving the existence of periodic patterns and localized structures. Future venues will include the study of the quantum spatial correlations present on (and between) the optical and mechanical fields, which may lead to noncritical squeezing and multipartite entanglement similarly to what has been found in optical parametric oscillators [20, 27].

We acknowledge fruitful discussions with Chiara Molinelli. This work has been supported by the Spanish Government and the European Union FEDER through Project FIS2011-26960. J.R.-R. is a grant holder of the FPU program of the Ministerio de Educación, Cultura y Deporte (Spain). C.N.-B. acknowledges the financial support of the Future and Emerging Technologies (FET) programme within the Seventh Framework Programme for Research of the European Commission, under the FET-Open grant agreement MALICIA, number FP7-ICT-265522.

Supplemental material

Derivation of the light field equation. In the following we deduce equation (3) of the main text. To this aim we use the approach of reference [22], which consists in propagating the complex amplitudes $A_{\pm}(z, \mathbf{r}, t)$ along a full cavity roundtrip, for what we assume that they are slowly varying in space and time so that they satisfies the paraxial wave equation

$$(\partial_z \pm c^{-1}\partial_t) A_{\pm} = \pm \frac{i}{2k_L} \nabla_{\perp}^2 A_{\pm}. \quad (15)$$

Given the amplitude $A_+(z = L, \mathbf{r}, t)$, after reflection on the deformable mirror we get $A_-(L, \mathbf{r}, t) e^{-ik_L L} = -\exp[2ik_L Q(\mathbf{r}, t)] A_+(L, \mathbf{r}, t) e^{ik_L L}$ where $Q(\mathbf{r}, t)$ represents the displacement of the mirror from its rest position ($Q = 0$ at rest). This amplitude $A_-(L, \mathbf{r}, t)$ propagates from $z = L$ to $z = 0$ giving rise to a new amplitude $A_-(0, \mathbf{r}, t + \frac{1}{2}t_c) = U_L A_-(L, \mathbf{r}, t)$, where $t_c = 2L/c$ is the cavity roundtrip time and $U_L = \exp[i(L/2k_L)\nabla^2]$ corresponds to the paraxial propagation operator in free space. After reflection onto the coupling mirror a new amplitude $A_+(0, \mathbf{r}, t + \frac{1}{2}t_c) = -\sqrt{R}A_-(0, \mathbf{r}, t + \frac{1}{2}t_c) + \sqrt{T}A_{\text{inj}}(0, \mathbf{r}, t + \frac{1}{2}t_c)$ is got, with R and T the reflectivity and transmissivity factors of the coupling mirror, respectively ($R + T = 1$ is assumed: lossless mirror). Finally propagation from $z = 0$ to $z = L$ yields $A_+(L, \mathbf{r}, t + t_c) = U_L A_+(0, \mathbf{r}, t + \frac{1}{2}t_c)$. Adding all parts together one gets

$$A(\mathbf{r}, t + t_c) = \sqrt{R}e^{2ik_L L} U_L^2 \exp[2ik_L Q(\mathbf{r}, t)] A(\mathbf{r}, t) + \sqrt{T}A_{\text{inj}}(L, \mathbf{r}, t + t_c), \quad (16)$$

where we used $U_L A_{\text{inj}}(0, \mathbf{r}, t + \frac{1}{2}t_c) = A_{\text{inj}}(L, \mathbf{r}, t + t_c)$. We now take into account that $R \rightarrow 1$ so that $\sqrt{R} = \sqrt{1 - T} \rightarrow 1 - \frac{1}{2}T$: Remember that T is very small. Next we assume that light is almost resonant with the cavity, specifically we impose that $2(\omega_L - \omega_c)L/c = \delta$ is of order T , where ω_c is the cavity longitudinal mode frequency (hence $\omega_c = m\pi c/L$, $m \in \mathbb{N}$) closest to ω_L , what allows approximating $\exp(2ik_L L) = \exp(2i\omega_L L/c) \approx 1 + i\delta$. We assume as well that $k_L Q(\mathbf{r}, t)$ is of order T (the mirror displacement/deformations are much smaller than the optical wavelength), so that $\exp[2ik_L Q(\mathbf{r}, t)] \approx$

$1 + 2ik_L Q(\mathbf{r}, t)$. Similarly we assume that the effect of diffraction is small (this implies that both mirrors must be sufficiently close each other, either physically or by means of lenses) so that we can expand $U_L^2 \approx 1 + i(L/k_L)\nabla_{\perp}^2$. All these assumptions imply that the overall variation of A between consecutive roundtrips is very small and then one can approximate $\partial_t A$ by $[A(\mathbf{r}, t + t_c) - A(\mathbf{r}, t)]t_c^{-1}$. With all these approximations we get, to the lowest nontrivial order,

$$\partial_t A(\mathbf{r}, t) = \gamma_c \left(-1 + i\Delta + i l_c^2 \nabla_{\perp}^2 + i \frac{4k_L}{T} Q \right) A + \gamma_c \mathcal{E}, \quad (17)$$

where $\gamma_c = T/2t_c = cT/4L$ is the cavity damping rate, $\Delta = (\omega_L - \omega_c)/\gamma_c$ is the dimensionless detuning parameter, $l_c^2 = 2L/k_L T$ is the diffraction length (squared), and $\mathcal{E}(\mathbf{r}, t) = 2T^{-1/2}A_{\text{inj}}(L, \mathbf{r}, t + t_c)$ is a scaled version of the injection field amplitude.

Details of the linear stability analysis. In the following we explain how we have performed the stability analysis of the homogeneous, stationary solution (12) given in the main text. We have followed the standard linear stability analysis, by studying the evolution of small perturbations $(\delta F, \delta Z)$ added to the steady solution (\bar{F}, \bar{Z}) . Upon linearizing the model equations (10) with respect to $(\delta F, \delta Z)$, expressing them in terms of the normal mode basis as $\delta F(\mathbf{r}', \tau) = \sum_{\mathbf{k}} \phi_{\mathbf{k}}(\tau) e^{i\mathbf{k} \cdot \mathbf{r}'}$ and $\delta Z(\mathbf{r}', \tau) = \sum_{\mathbf{k}} \zeta_{\mathbf{k}}(\tau) e^{i\mathbf{k} \cdot \mathbf{r}'}$ (note that $\zeta_{-\mathbf{k}}^* = \zeta_{\mathbf{k}}$ because δZ is a real field), and equating coefficients of like exponentials, we get, for each \mathbf{k} , a linear system of differential equations for the modal perturbations $\mathbf{v} \equiv (\phi_{\mathbf{k}}, \phi_{-\mathbf{k}}^*, \zeta_{\mathbf{k}})$. Owing to this linearity and the time invariance of the system, its solutions have the form $\mathbf{v}(\tau) = \mathbf{v}(0) e^{\lambda \tau}$. Upon making such substitution a homogeneous linear system of algebraic equations in $\mathbf{v}(0)$ is got, whose condition for existence of nontrivial solutions reads $C(k^2; \lambda) \equiv \sum_{n=0}^4 c_n(k^2) \lambda^n = 0$, where k is the modulus of \mathbf{k} . After simple algebra we get $c_4 = 1$, $c_3 = 2 + \gamma$, and

$$c_2 = 1 + 2\gamma + \Omega_k^2 + (\Delta_k + \bar{I})^2, \quad (18a)$$

$$c_1 = \gamma \left[1 + (\Delta_k + \bar{I})^2 \right] + 2\Omega_k^2, \quad (18b)$$

$$c_0 = 2\bar{I}(\Delta_k + \bar{I})\Omega_0^2 + \left[1 + (\Delta_k + \bar{I})^2 \right] \Omega_k^2, \quad (18c)$$

where $\Omega_k^2 \equiv \Omega_0^2(1 + \rho^2 k^2)$ and $\Delta_k \equiv \Delta - k^2$. We observe that the growth exponents λ , solutions to $C(k^2; \lambda) = 0$, depend on k and not on \mathbf{k} because of the rotational invariance of both the steady state and the model equations. Whenever $\text{Re}\{\lambda\} < 0$ for all k the steady state is stable, while if $\text{Re}\{\lambda\} > 0$ for some k it is unstable. The condition $\text{Re}\{\lambda\} = 0$ thus defines a possible instability, or bifurcation, which is met either when $\lambda = 0$ (static instability: $c_0 = 0$) or when $\lambda = i\sqrt{c_1/c_3}$ (self-pulsing, or Hopf instability: $c_1 c_2 c_3 = c_4 c_1^2 + c_3^2 c_0$). On the other hand, when the bifurcation is associated with $k = 0$ the

new state is spatially uniform (homogeneous instability), while if $k \neq 0$ the instability is pattern forming.

-
- [1] J. M. Raimond, M. Brune, and S. Haroche, *Rev. Mod. Phys.* **73**, 565 (2001); H. Walther, B. T. H. Varcoe, B.-G. Englert, and Th. Becker, *Rep. Prog. Phys.* **69**, 1325 (2006).
 - [2] D. Jaksch and P. Zoller, *Ann. Phys.* **315**, 52 (2004); M. Lewenstein, A. Sanpera, and V. Ahufinger, *Ultracold Atoms In Optical Lattices: Simulating Quantum Many-body Systems* (Oxford University Press, USA, 2012)
 - [3] D. Leibfried, R. Blatt, C. Monroe, and D. Wineland, *Rev. Mod. Phys.* **75**, 281 (2003); Ch. Schneider, D. Porras, and T. Schaetz, *Rep. Prog. Phys.* **75**, 024401 (2012).
 - [4] M. H. Devoret, A. Wallraff, and J. M. Martinis, *arXiv:cond-mat/0411174v1* [cond-mat.mes-hall]; J. Q. You and F. Nori, *Phys. Today* **58**, 42 (2005).
 - [5] B. Urbaszek, X. Marie, T. Amand, O. Krebs, P. Voisin, P. Maletinsky, A. Hoge, and A. Imamoglu, *arXiv:1202.4637* [cond-mat.mes-hall].
 - [6] K. Hammerer, A. S. Sørensen, and E. S. Polzik, *Rev. Mod. Phys.* **82**, 1041 (2010); C. A. Muschik, H. Krauter, K. Hammerer, and E. S. Polzik, *Quantum Info. Process.* **10**, 839 (2011).
 - [7] T. J. Kippenberg and K. J. Vahala, *Opt. Exp.* **15**, 17172 (2007); F. Marquardt and S. M. Girvin, *Physics* **2**, 40 (2009).
 - [8] A. Dorsel, J. D. McCullen, P. Meystre, E. Vignes, and H. Walther, *Phys. Rev. Lett.* **51**, 1550 (1983); P. Maystre, E. M. Wright, J. D. McCullen, and E. Vignes, *J. Opt. Soc. Am. B* **2**, 1830 (1985).
 - [9] L. A. Lugiato and R. Lefever, *Phys. Rev. Lett.* **58**, 2209–2211 (1987).
 - [10] T. J. Kippenberg, H. Rokhsari, T. Carmon, A. Scherer, and K. J. Vahala, *Phys. Rev. Lett.* **95**, 033901 (2005); O. Arcizet, P.-F. Cohadon, T. Briant, M. Pinard, and A. Heidmann, *Nature* **444**, 71 (2006); A. Schliesser, P. Del’Haye, N. Nooshi, K. J. Vahala, and T. J. Kippenberg, *Phys. Rev. Lett.* **97**, 243905 (2006).
 - [11] S. Weis, R. Rivière, S. Deléglise, E. Gavartin, O. Arcizet, A. Schliesser, and T. J. Kippenberg, *Science* **330**, 1520 (2010); J. D. Teufel, D. Li, M. S. Allman, K. Cicak, A. J. Sirois, J. D. Whittaker, and R. W. Simmonds, *Nature* **471**, 204 (2011); A. H. Safavi-Naeini, T. P. Mayer Alegre, J. Chan, M. Eichenfield, M. Winger, Q. Lin, J. T. Hill, D. E. Chang, and O. Painter, *Nature* **472**, 69 (2011).
 - [12] G. Heinrich, M. Ludwig, J. Qian, B. Kubala, and F. Marquardt, *Phys. Rev. Lett.* **107**, 043603 (2011).
 - [13] F. Marino and F. Marin, *Phys. Rev. E* **83**, 015202(R) (2011).
 - [14] A. Butsch, C. Conti, F. Biancalana, and P. St. J. Russell, *Phys. Rev. Lett.* **108**, 093903 (2012); C. Conti, A. Butsch, F. Biancalana, and P. St. J. Russell, *Phys. Rev. A* **86**, 013830 (2012).
 - [15] E. Tesio, G. R. M. Robb, T. Ackemann, W. J. Firth, and G.-L. Oppo, *Phys. Rev. A* **86**, 031801(R) (2012).
 - [16] R. Horodecki, P. Horodecki, M. Horodecki, and Karol Horodecki, *Rev. Mod. Phys.* **81**, 865 (2009).
 - [17] O. Pfister, S. Feng, G. Jennings, R. Pooser, and D. Xie, *Phys. Rev. A* **70**, 020302(R) (2004); N. C. Menicucci, S. T. Flammia, H. Zaidi, and O. Pfister, *Phys. Rev. A* **76**, 010302(R) (2007); M. Pysher, Y. Miwa, R. Shahrokhshahi, R. Bloomer, and O. Pfister, *Phys. Rev. Lett.* **107**, 030505 (2011); R. Shahrokhshahi and O. Pfister, *Quant. Inf. Comp.* **12**, 0953 (2012).
 - [18] G. Patera, C. Navarrete-Benlloch, G. J. de Valcárcel, and C. Fabre, *Eur. Phys. J. D* **66**, 241 (2012).
 - [19] K. Staliunas and V. J. Sánchez-Morcillo, *Transverse Patterns in Nonlinear Optical Resonators*, (Springer, Berlin, 2003).
 - [20] L. A. Lugiato and G. Grynberg, *Europhys. Lett.* **29**, 675 (1995); L. A. Lugiato and A. Gatti, *Phys. Rev. Lett.* **70**, 3868 (1993); A. Gatti and L. A. Lugiato, *Phys. Rev. A* **52**, 1675 (1995); I. Pérez-Arjona, E. Roldán, and G. J. de Valcárcel, *Europhys. Lett.* **74**, 247 (2006); *Phys. Rev. A* **75**, 063802 (2007).
 - [21] In the following we choose $\mathcal{V} = \frac{1}{2}\sqrt{\hbar\omega_c/\varepsilon_0 L}$ in order to make contact with quantum optics when necessary, as in this way the quantized field verifies the standard equal-time commutation relation $[A(\mathbf{r}, t), A^\dagger(\mathbf{r}', t)] = \delta^2(\mathbf{r} - \mathbf{r}')$.
 - [22] S. Kolpakov, A. Esteban-Martín, F. Silva, J. García, K. Staliunas, and G. J. de Valcárcel, *Phys. Rev. Lett.* **101**, 254101 (2008).
 - [23] M. Pinarda, Y. Hadjarb, and A. Heidmann, *Eur. Phys. J. D* **7**, 107 (1999).
 - [24] According to [21] $\langle S_+ \rangle = \hbar\omega_c |A(\mathbf{r}, t)|^2 / t_c$, hence $|A(\mathbf{r}, t)|^2$ has the meaning of number of photons impinging the deformable mirror per unit area during a cavity roundtrip time.
 - [25] I. Pérez-Arjona, F. Silva, E. Roldán, and G. J. de Valcárcel, *Opt. Express* **12**, 2130 (2004).
 - [26] L. M. Narducci and N. B. Abraham, *Laser Physics and Laser Instabilities* (World Scientific, Singapore, 1988); I. S. Gradshteyn, and I. M. Ryzhik, "Routh-Hurwitz Theorem." §15.715 in *Tables of Integrals, Series, and Products*, 6th ed., p. 1076 (Academic Press, San Diego, CA, 2000).
 - [27] C. Navarrete-Benlloch, E. Roldán, and G. J. de Valcárcel, *Phys. Rev. Lett.* **100**, 203601 (2008); C. Navarrete-Benlloch, G. J. de Valcárcel, and E. Roldán, *Phys. Rev. A* **79**, 043820 (2009); C. Navarrete-Benlloch, A. Romanelli, E. Roldán, and G. J. de Valcárcel, *Phys. Rev. A* **81**, 043829 (2010).